

Power Exhaust in JET MkIIGB ELMy H-modes

W.Fundamenski, G.Matthews, V.Riccardo, T.Eich¹, C.Ingesson³, T.Kiviniemi², T.Kurki-Suonio², V.Philipps¹, S.Sipilä², and contributors to the EFDA-JET workprogramme

Euratom/UKAEA Fusion Association, Culham Science Centre, Abingdon, Oxon, UK

¹*FZ Julich GmbH/Euratom, Institut für Plasmaphysik, TEC, D-52425 Julich, Germany*

²*Helsinki U. of Technology, Euratom-TEKES Assoc., PO Box 2200, FIN-02015 HUT, Finland*

³*FOM-Rijnhuizen, Ass. Euratom-FOM, TEC, PO Box 1207, 3430 BE Nieuwegein, NL*

1. Motivation and Description of the Experiment

The exhaust of power from a tokamak plasma is one of the key constraints on the design of a fusion reactor. The ITER divertor was designed on the basis of infra-red (IR) thermographic measurements of power deposition profiles in D-IIID, ASDEX-U and JT-60U, which indicate a broadening of the power profile with input power^{1,2}. Recently a novel technique was developed at JET to measure time averaged power profiles using thermocouples (TC) embedded in the MkIIGB divertor plates. In its original form it involved the lifting of the strike point over a junction between vertical tiles on a shot-by-shot basis and inferring the power deposition profile as the spatial derivative of the partition of energy between the two tiles³. This method was very robust but too costly in shots for general application. For this reason an alternative method was developed involving the sweeping of the strike point over a thermocouple location within a single discharge and extracting the power profile using a finite-element model of the tile⁴, Figs.1-2 (the two methods agree quite well at the outer target). Both methods indicate much narrower power profiles (higher peak wall loads) in high power ELMy H-modes, and the interpretation of this result is the main aim of the paper.

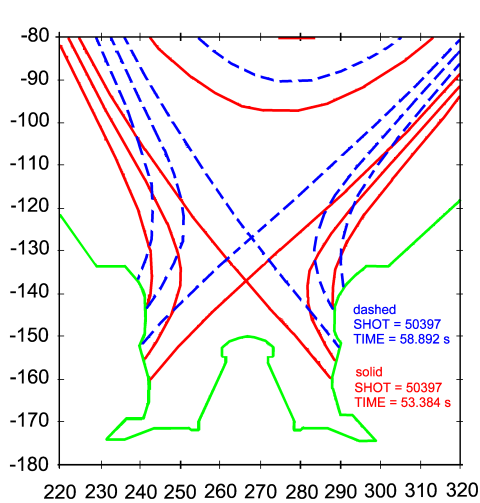


Fig.1: Initial and final positions of the vertical sweep used in the TC method

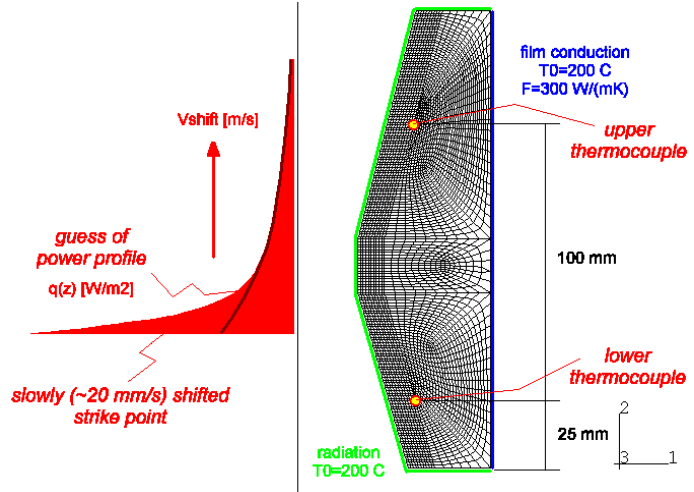


Fig.2. Finite element model of the outer vertical tile and adjustable double exponential profile

2. Results and Analysis

Power deposition profiles were measured using the latter method in a series of 2.5MA/2.4T discharges involving a scan in the NBI heating power (4-18 MW, where $P_{L-H} \sim 5$ MW) and a scan in D_2 fuelling rate ($0-3 \times 10^{22} \text{ s}^{-1}$). The outer peak heat flux is roughly five times larger than the inner one, Fig.3, so that the following discussion will focus on the outer target only. In L-mode, the heat flux decays exponentially away from the strike point, while in H-mode, a double exponential structure appeared on the outer target only, with a narrow e-folding length

near the separatrix (~ 3 mm mapped to outer mid-plane) and a broader base profile elsewhere in the scrape-off-layer (~ 5 -7 mm-omp). Without gas puffing, the narrow layer was found to scale inversely with power entering the SOL, $\lambda_{q,nw} \propto P_{SOL}^{-0.4 \pm 0.1}$, while the base profile showed virtually no power dependence. At constant input power (12 MW), the peak heat flux was strongly reduced by D₂ puffing (from ~ 20 to 4 MW/m²), with the narrow feature in the power profile effectively suppressed. Comparison of the total power profile (from TC analysis) with the electron power profile from Langmuir probes (LP), allowed the calculation of the ion power profile. Decomposition into the ion and electron channels, and into the double exponential (thin-wide) components, revealed a strong correspondence of the narrow layer with the ions, and of the base profile with the electrons, Figs.4-5 (here parallel heat flux is shown, where $q_{||}/q_{target} \sim 13$). The peak heat flux was dominated by the ions for $P_{SOL} > 8$ MW (no gas puff) and for D₂ puff rate $< 10^{22} \text{ s}^{-1}$ (12 MW).

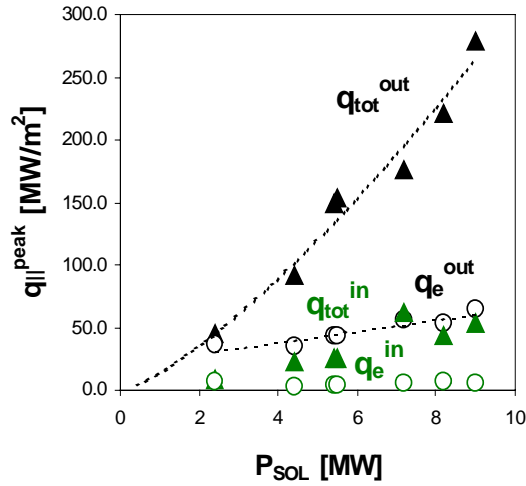


Fig.3. Total and electron peak heat flux values at the outer and inner targets; power scan.

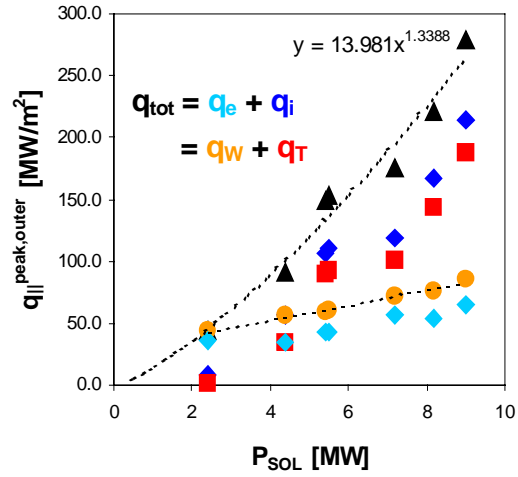


Fig.4. Outer peak heat flux in terms of the ion-electron and thin-wide components

Regression analysis of both scans led to the following scaling for the integral power width, $\lambda_{q,int} \propto P_{SOL}^{-0.4 \pm 0.1} n_{sep}^{+0.4 \pm 0.1}$, which is in sharp contrast to the ITER-99 scaling, $\lambda_{q,int} \propto P_{SOL}^{+0.35 \pm 0.1}$. Comparison of $\lambda_{q,int}^{JET-TC}$ with various theoretical models suggests neo-classical transport in the SOL, Fig.6 (for some effects, the pedestal density may be more relevant).

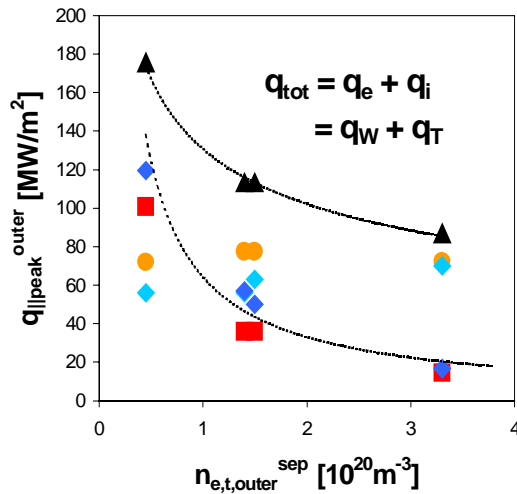


Fig.5. Similar to Fig.4, only for the gas puff (target density) scan

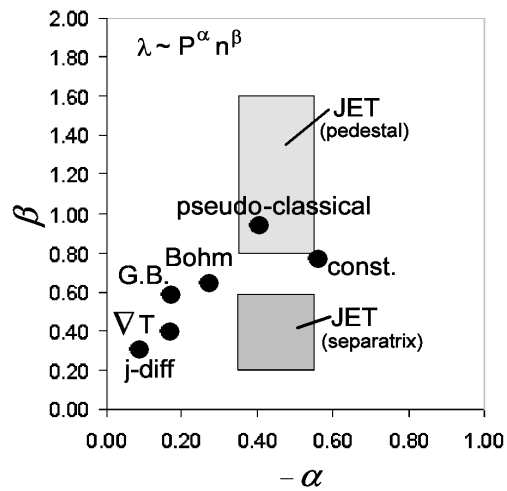


Fig.6. Comparison of various theories of SOL transport with the obtained scaling

3. Modelling and Interpretation

Modelling the SOL plasma using the OSM2/EIRENE coupled codes^{5,6} lead to the following conclusions: a) Fluid modelling is insufficient to explain the observed asymmetry in the peak heat flux, b) in order to obtain global power balance, a ratio of ion to electron power entering the SOL of roughly 10 is required, c) although electrons remain collisional, $v_e^* \sim 10-20$, the ions become collisionless $v_i^* \sim 1-2$ near the separatrix, d) the extracted radial heat diffusivities fall to neo-classical levels near the separatrix. Based on these results, ion orbit loss from the pedestal region was suggested as a candidate mechanism for explaining the narrow feature in the power deposition profile⁷. The ASCOT code⁸ was used to investigate this effect using a three stage analysis: a) trace calculations on specified JET equilibria, b) self-consistent simulations with realistic pedestal profiles, c) grid based, coupled-code (ASCOT-OSM2/EIRENE) simulations, with reconstructed 2-D SOL distribution of ions, electrons and neutrals. ASCOT is a 3-D Monte-Carlo guiding centre code, including all neo-classical effects (all drift terms) as well as ion-ion and ion-neutral collisions. Here we only present the final results. The inner and outer ion power deposition profiles obtained with ASCOT for the case without the SOL plasma and for various levels of the radial electric field in the SOL are shown in Fig.7a. Similar profiles with the SOL plasma from OSM2/EIRENE reconstruction are shown in Fig.7b. The effect of E_r is to increase the outer/inner asymmetry via the ExB drift, while SOL losses reduce the peak heat flux by $\sim 50\%$. The estimated E_r value for this shot was $\sim 30-100$ kV/m, while the inner and outer peak ion heat flux estimates based on TC/LP analysis were 9.4 and 4.5 MW/m². These values agree with the ASCOT estimate for $E_r \sim 55$ kV/m which is consistent with the field range cited above, although the profiles are even more narrow than observed experimentally. This could be due to interaction with the fluctuating E-fields which so far has not be included in the model

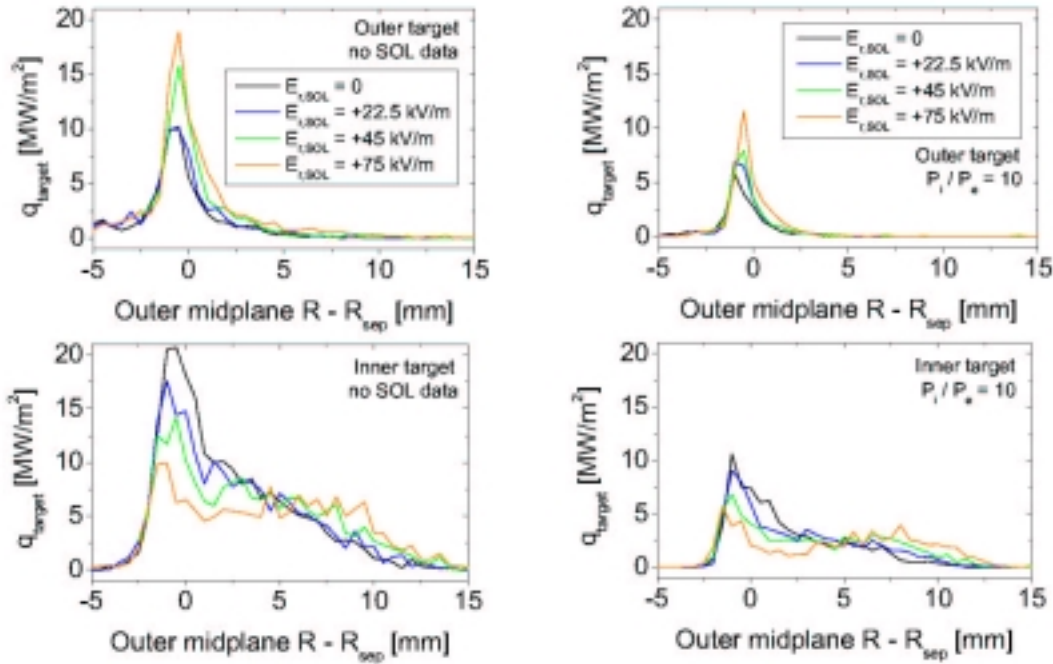


Fig.7. ASCOT target power profiles mapped to the outer mid-plane, for four levels of the radial electric field. On the left (a) is the no-SOL case, on the right (b) SOL with $P_i/P_e = 10$.

4. Comparison of LP, TC and IR profiles

Preliminary infra-red thermographic⁹ profiles of power deposition (obtained with the ABAQUS code) on the outer target differ visibly from both the TC & LP profiles, Fig.8. The difference is more pronounced in the H-mode case, where both the TC & LP profiles are narrower than in the L-mode and skewed towards the SOL, while the IR profile remains roughly symmetric and of the same width as in the L-mode. It should be emphasised that the IR diagnostic is operating close to its spatial resolution limit (one pixel ~ 7 mm in Fig.8). Methods of improving the spatial resolution by analysing swept shots are being considered.

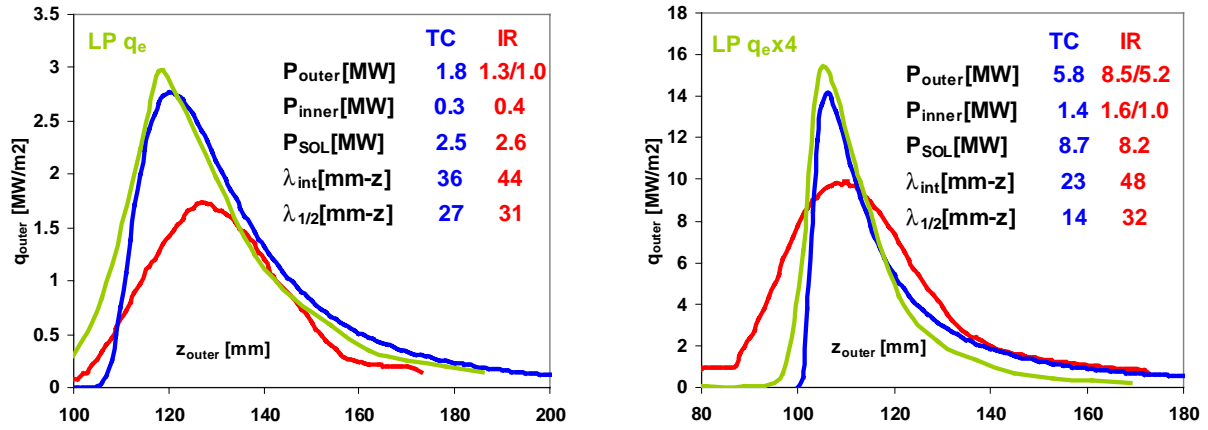


Fig.8. Comparison of Langmuir probe (LP), Thermocouple (TC) and Infra-Red (IR) profiles for 4 MW L-mode (left) and 16 MW H-mode (right).

5. Conclusions and Consequences for ITER

The narrow feature in the power deposition profile, first observed in Ref.3, was confirmed by the new diagnostic technique, and modelling indicates that ion orbit losses are a probable cause of this effect. The profile width was found to decrease with input power and increase with separatrix density according to $\lambda_{q,int} \propto P_{SOL}^{-0.4 \pm 0.1} n_{sep}^{+0.4 \pm 0.1}$, in disagreement with the ITER-99 scaling. This new scaling predicts rather narrow power width in ITER (with neo-classical R and B dependence, $\lambda_{q,int} \sim 2.2 - 4.4$ mm vs. ~ 15 mm with the ITER-99 scaling), but this is probably ameliorated by the higher neutral density in the ITER divertor which reduce orbit loss ion energy via charge exchange scattering; ASCOT simulations are planned to address this point. However, it is clear that due to lower upstream collisionality ($v_{i,sep}^* \sim 0.5-1$), ion orbit losses will play an important role in ITER SOL and divertor physics.

This work was conducted under European Fusion Development Agreement and was partly funded by EURATOM and the UK Department of Trade and Industry.

- [1] ITER database, many authors, *Nuclear Fusion*, **39** (1999), 2423.
- [2] A.Loarte, *J. Nucl. Materials*, **266-269** (1999), 99.
- [3] G.F.Matthews et al., *J. Nucl. Materials*, **290-293** (2001), 668.
- [4] V.Riccardo et al., *Plasma Phys. Contr. Fusion*, **43** (2001), 1.
- [5] W.Fundamenski, Ph.D. Thesis, U.Toronto (1999).
- [6] D.Reiter, *J.Nucl. Materials*, **196-198** (1992), 80.
- [7] W.Fundamenski, *J. Nucl. Materials*, **290-293** (2001), 593.
- [8] J.A.Heikkinen, *Phys.Plasma*, **8** (2001), 2824.
- [9] T.Eich et al., "Analysis of Power deposition in JET MkIIIGB divertor by IR-thermography", these proceedings.